

Status and Perspective of the DarkSide Experiment at LNGS

P. AGNES⁽¹⁾, L. AGOSTINO⁽²⁾, I. F. M. ALBUQUERQUE⁽³⁾, T. ALEXANDER⁽⁴⁾,
 A. K. ALTON⁽⁵⁾, D. M. ASNER⁽⁴⁾, H. O. BACK⁽⁴⁾, B. BALDIN⁽⁶⁾, K. BIERY⁽⁶⁾,
 V. BOCCI⁽⁴¹⁾, G. BONFINI⁽⁹⁾, W. BONIVENTO⁽¹⁷⁾, M. BOSSA⁽¹⁰⁾⁽⁹⁾, B. BOTTINO⁽¹¹⁾⁽¹²⁾,
 A. BRIGATTI⁽¹³⁾, J. BRODSKY⁽⁷⁾, F. BUDANO⁽¹⁴⁾⁽¹⁵⁾, S. BUSSINO⁽¹⁴⁾⁽¹⁵⁾, M. CADEDDU⁽¹⁶⁾⁽¹⁷⁾,
 M. CADONI⁽¹⁶⁾⁽¹⁷⁾, F. CALAPRICE⁽⁷⁾, N. CANCI⁽¹⁾⁽⁹⁾, A. CANDELA⁽⁹⁾, M. CARAVATI⁽¹⁶⁾⁽¹⁷⁾,
 M. CARIELLO⁽¹²⁾, M. CARLINI⁽⁹⁾, S. CATALANOTTI⁽¹⁹⁾⁽¹⁸⁾, P. CAVALCANTE⁽²⁰⁾⁽⁹⁾,
 A. CHEPURNOV⁽²¹⁾, C. CICALÒ⁽¹⁷⁾, A. G. COCCO⁽¹⁸⁾, G. COVONE⁽¹⁹⁾⁽¹⁸⁾, D. D'ANGELO⁽²²⁾⁽¹³⁾,
 M. D'INCECCO⁽⁹⁾, S. DAVINI⁽¹²⁾⁽¹⁰⁾, S. DE CECCO⁽⁴²⁾, M. DE DEO⁽⁹⁾, M. DE VINCENZI⁽¹⁴⁾⁽¹⁵⁾,
 A. V. DERBIN⁽²³⁾, A. DEVOTO⁽¹⁶⁾⁽¹⁷⁾, F. DI EUSANIO⁽⁷⁾, G. DI PIETRO⁽⁹⁾⁽¹³⁾,
 C. DIONISI⁽⁴¹⁾⁽⁴²⁾, E. EDKINS⁽²⁴⁾, A. EMPL⁽¹⁾, A. FAN⁽²⁵⁾, G. FIORILLO⁽¹⁹⁾⁽¹⁸⁾,
 K. FOMENKO⁽²⁷⁾, D. FRANCO⁽²⁶⁾, F. GABRIELE⁽⁹⁾, C. GALBIATI⁽⁷⁾⁽¹³⁾, S. GIAGU⁽⁴¹⁾⁽⁴²⁾,
 C. GIGANTI⁽²⁾, G. K. GIOVANETTI⁽⁷⁾, A. M. GORETTI⁽⁹⁾, F. GRANATO⁽²⁸⁾, M. GROMOV⁽²¹⁾,
 M. GUAN⁽²⁹⁾, Y. GUARDINCERRI^{(6)(*)}, B. R. HACKETT⁽²⁴⁾, K. HERNER⁽⁶⁾, D. HUGHES⁽⁷⁾,
 P. HUMBLE⁽⁴⁾, E. V. HUNGERFORD⁽¹⁾, AL. IANNI⁽³⁰⁾⁽⁹⁾, AN. IANNI⁽⁷⁾⁽⁹⁾, I. JAMES⁽¹⁴⁾⁽¹⁵⁾,
 T. N. JOHNSON⁽³⁸⁾, C. JOLLET⁽³¹⁾, K. KEETER⁽³²⁾, C. L. KENDZIORA⁽⁶⁾, G. KOH⁽⁷⁾,
 D. KORABLEV⁽²⁷⁾, G. KORGA⁽¹⁾⁽⁹⁾, A. KUBANKIN⁽³³⁾, X. LI⁽⁷⁾, M. LISSIA⁽¹⁷⁾,
 B. LOER⁽⁴⁾, P. LOMBARDI⁽¹³⁾, G. LONGO⁽¹⁹⁾⁽¹⁸⁾, Y. MA⁽²⁹⁾, A. A. MACHADO⁽⁴⁰⁾,
 I. N. MACHULIN⁽³⁴⁾⁽³⁵⁾, A. MANDARANO⁽¹⁰⁾⁽⁹⁾, S. M. MARI⁽¹⁴⁾⁽¹⁵⁾, J. MARICIC⁽²⁴⁾,
 L. MARINI⁽¹¹⁾⁽¹²⁾, C. J. MARTOFF⁽²⁸⁾, A. MEREGAGLIA⁽³¹⁾, P. D. MEYERS⁽⁷⁾,
 R. MILINCIC⁽²⁴⁾, J. D. MILLER⁽¹⁾, A. MONTE⁽⁸⁾, B. J. MOUNT⁽³²⁾, V. N. MURATOVA⁽²³⁾,
 P. MUSICO⁽¹²⁾, J. NAPOLITANO⁽²⁸⁾, A. NAVRER AGASSON⁽²⁾, A. OLEINIK⁽³³⁾, M. ORSINI⁽⁹⁾,
 F. ORTICA⁽³⁶⁾⁽³⁷⁾, L. PAGANI⁽³⁸⁾, M. PALLAVICINI⁽¹¹⁾⁽¹²⁾, E. PANTIC⁽³⁸⁾, S. PARMEGGIANO⁽¹³⁾,
 K. PELCZAR⁽³⁹⁾, N. PELLICCIA⁽³⁶⁾⁽³⁷⁾, A. POCAR⁽⁸⁾, S. PORDES⁽⁶⁾, D. A. PUGACHEV⁽³⁴⁾,
 H. QIAN⁽⁷⁾, K. RANDLE⁽⁷⁾, G. RANUCCI⁽¹³⁾, M. RAZETI⁽¹⁷⁾, A. RAZETO⁽⁹⁾⁽⁷⁾,
 B. REINHOLD⁽²⁴⁾, A. L. RENSHAW⁽¹⁾, M. RESCIGNO⁽⁴¹⁾, Q. RIFFARD⁽²⁶⁾, A. ROMANI⁽³⁶⁾⁽³⁷⁾,
 B. ROSSI⁽¹⁸⁾, N. ROSSI⁽⁹⁾, D. SABLONE⁽⁷⁾⁽⁹⁾, P. SAGGESE⁽¹³⁾, W. SANDS⁽⁷⁾, C. SAVARESE⁽¹⁰⁾⁽⁹⁾,
 B. SCHLITZER⁽³⁸⁾, E. SEGRETO⁽⁴⁰⁾, D. A. SEMENOV⁽²³⁾, P. N. SINGH⁽¹⁾, M. D. SKOROKHVATOV⁽³⁴⁾⁽³⁵⁾,
 O. SMIRNOV⁽²⁷⁾, A. SOTNIKOV⁽²⁷⁾, C. STANFORD⁽⁷⁾, Y. SUVOROV⁽²⁵⁾⁽⁹⁾⁽³⁴⁾, R. TARTAGLIA⁽⁹⁾,
 G. TESTERA⁽¹²⁾, A. TONAZZO⁽²⁶⁾, P. TRINCHESE⁽¹⁹⁾⁽¹⁸⁾, E. V. UNZHAKOV⁽²³⁾,
 M. VERDUCCI⁽⁴¹⁾⁽⁴²⁾, A. VISHNEVA⁽²⁷⁾, B. VOGELAAR⁽²⁰⁾, M. WADA⁽⁷⁾, S. WALKER⁽¹⁹⁾⁽¹⁸⁾,
 H. WANG⁽²⁵⁾, Y. WANG⁽²⁹⁾⁽²⁵⁾, A. W. WATSON⁽²⁸⁾, S. WESTERDALE⁽⁷⁾, J. WILHELMI⁽²⁸⁾,
 M. M. WOJCIK⁽³⁹⁾, X. XIANG⁽⁷⁾, X. XIAO⁽²⁵⁾, J. XU⁽⁷⁾, C. YANG⁽²⁹⁾, Z. YE⁽¹⁾,
 W. ZHONG⁽²⁹⁾, C. ZHU⁽⁷⁾, G. ZUZEL⁽³⁹⁾
 (THE DARKSIDE COLLABORATION)

⁽¹⁾ Dept. of Physics, University of Houston, Houston, TX 77204, USA

⁽²⁾ LPNHE Paris, Université Pierre et Marie Curie, CNRS/IN2P3, Paris 75252, France

⁽³⁾ Inst. de Física, Universidade de São Paulo, São Paulo 05508-090, Brazil

(*) Deceased

- (⁴) *Pacific Northwest National Laboratory, Richland, WA 99354, USA*
- (⁵) *Dept. of Physics, Augustana University, Sioux Falls, SD 57197, USA*
- (⁶) *Fermi National Accelerator Laboratory, Batavia, IL 60510, USA*
- (⁷) *Dept. of Physics, Princeton University, Princeton, NJ 08544, USA*
- (⁸) *Amherst Center for Fundamental Interactions and Dept. of Physics, University of Massachusetts, Amherst, MA 01003, USA*
- (⁹) *Laboratori Nazionali del Gran Sasso, Assergi AQ 67010, Italy*
- (¹⁰) *Gran Sasso Science Inst., L'Aquila 67100, Italy*
- (¹¹) *Dept. of Physics, Università degli Studi, Genova 16146, Italy*
- (¹²) *INFN, Sezione di Genova, Genova 16146, Italy*
- (¹³) *INFN, Sezione di Milano, Milano 20133, Italy*
- (¹⁴) *INFN, Sezione di Roma Tre, Roma 00146, Italy*
- (¹⁵) *Dept. of Physics and Mathematics, Università degli Studi Roma Tre, Roma 00146, Italy*
- (¹⁶) *Dept. of Physics, Università degli Studi, Cagliari 09042, Italy*
- (¹⁷) *INFN, Sezione di Cagliari, Cagliari 09042, Italy*
- (¹⁸) *INFN, Sezione di Napoli, Napoli 80126, Italy*
- (¹⁹) *Dept. of Physics, Università degli Studi Federico II, Napoli 80126, Italy*
- (²⁰) *Dept. of Physics, Virginia Tech, Blacksburg, VA 24061, USA*
- (²¹) *Skobeltsyn Inst. of Nucl. Physics, Lomonosov Moscow State University, Moscow 119991, Russia*
- (²²) *Dept. of Physics, Università degli Studi, Milano 20133, Italy*
- (²³) *St. Petersburg Nucl. Physics Inst. NRC Kurchatov Inst., Gatchina 188350, Russia*
- (²⁴) *Dept. of Physics and Astronomy, University of Hawaii, Honolulu, HI 96822, HI*
- (²⁵) *Dept. of Physics and Astronomy, University of California, Los Angeles, CA 90095, USA*
- (²⁶) *APC, Université Paris Diderot, CNRS/IN2P3, CEA/Irfu, Obs de Paris, USPC, 75205 Paris, France*
- (²⁷) *Joint Inst. for Nucl. Research, Dubna 141980, Russia*
- (²⁸) *Dept. of Physics, Temple University, Philadelphia, PA 19122, USA*
- (²⁹) *Inst. for High Energy Physics, Beijing 100049, China*
- (³⁰) *Laboratorio Subterráneo de Canfranc, Canfranc Estación E-22880, Spain*
- (³¹) *IPHC,19 Université de Strasbourg, CNRS/IN2P3, Strasbourg 67037, France*
- (³²) *School of Natural Sciences, Black Hills State University, Spearfish, SD 57799, USA*
- (³³) *Radiation Physics Laboratory, Belgorod National Research University, Belgorod 308007, Russia*
- (³⁴) *National Research Centre Kurchatov Institute, Moscow 123182, Russia*
- (³⁵) *National Research Nucl. University, MEPhI, Moscow 115409, Russia*
- (³⁶) *Dept. of Chemistry, Biology and Biotechnology, Università degli Studi, Perugia 06123, Italy*
- (³⁷) *INFN, Sezione di Perugia, Perugia 06123, Italy*
- (³⁸) *Dept. of Physics, University of California, Davis, CA 95616, USA*
- (³⁹) *Smoluchowski Inst. of Physics, Jagiellonian University, Krakow 30059, Poland*
- (⁴⁰) *Inst. of Physics Gleb Wataghin, Universidade Estadual de Campinas, São Paulo 13083-859, Brazil*
- (⁴¹) *INFN, Sezione di Roma, Roma 00185, Italy*
- (⁴²) *Physics Dept., Sapienza Università di Roma, Roma 00185, Italy*

Summary. — The DarkSide experiment aims to perform a background-free direct search for dark matter with a dual-phase argon TPC. The current phase of the experiment, DarkSide-50, is acquiring data at *Laboratori Nazionali del Gran Sasso* and produced the most sensitive limit on the WIMP-nucleon cross section ever obtained with a liquid argon target ($2.0 \times 10^{-44} \text{ cm}^2$ for a WIMP mass of $100 \text{ GeV}/c^2$). The future phase of the experiment will be a 20 t fiducial mass detector, designed to reach a sensitivity of $\sim 1 \times 10^{-47} \text{ cm}^2$ (at $1 \text{ TeV}/c^2$ WIMP mass) with a background-free exposure of 100 ty. This work contains a discussion of the current status of the DarkSide-50 WIMP search and of the results which are more relevant for the construction of the future detector.

PACS numbers: 29.40.Gx, 95.35.+d, 95.55.Vj

1. – Introduction

Dark matter represents 23% of the energy content of the Universe [1], but its particle nature remains unknown. One of the most favored candidate is a referred as *Weakly Interacting Massive Particle*, or WIMP. Dark matter can be searched for in indirect ways, as the production at colliders or the detection of the decay products of the WIMP self-annihilation. The direct detection channel exploits, on the other hand, the elastic scattering of WIMPs off ordinary nuclei. Direct detection experiments are improving year by year the sensitivity to (and the upper limit on) the WIMP-nucleon cross section in a wide range of WIMP masses (from $1 \text{ GeV}/c^2$ to $1000 \text{ TeV}/c^2$). A successful experiment requires a low energy threshold, since a typical WIMP induced nuclear recoil deposits a few tens of keV in the medium, and strong background rejection. The background levels are typically reduced by building the experiments in underground facilities. Further suppression is achieved by means of topological reconstruction of the interaction and, when available, Pulse Shape Discrimination (to distinguish β - and γ -induced electron recoils from nuclear recoils).

2. – The Choice of Liquid Argon

Noble liquids are suitable for direct dark matter searches. Any interaction inside the medium produces ionization and prompt scintillation light, which is due to de-excitation of excimers and recombined pairs. The high ionization and scintillation yields, purity and transparency to scintillation light allow to easily scale the size of a target up to large masses. Some xenon-based experiments are currently reaching the ton-scale size (Panda-X-II [2] and XENON-1t [3] are currently taking data at Jinping Lab and LNGS respectively and the construction of the LZ detector [4] is about to start). These experiments share the dual-phase TPC design, where a gas layer is created on top of the liquid active volume. One or more arrays of photo-detectors are used to trigger on and collect the prompt scintillation signal (S1). The sensitive volume is then immersed in a uniform electric field, to drift the ionization electrons up to the gaseous region. The extraction and acceleration of the free electrons in the gas induces a second light emission (called S2, by proportional electro-luminescence). Thanks to the light patten on the top array

of photo-detectors it is possible to reconstruct the interaction position in the $x - y$ plane, while the time difference between S2 and S1 is proportional to the drift distance along the vertical axis.

Dual-phase TPCs allow to reject the background thanks to this full 3D position reconstruction. A WIMP is expected to interact only once in the sensitive volume, while neutrons and gammas are likely to produce multiple interactions, resulting in multiple S2 events. Moreover, fiducialization can be applied to remove surface events. In addition to this, the ratio between ionization and scintillation is different for electron recoils (ERs) and nuclear recoils (NRs). This features guarantees a rejection power of the order of 10^3 .

Liquid argon offers an additional and very powerful tool for electron recoil discrimination, based on the shape of the scintillation pulse. A noble liquid atom has two states, excited in different proportion if the recoiling species is an electron or a nucleus. The typical fraction of singlet state is 0.3 (0.7) for ER (NR) at energy larger than few tens of keV. Since the two decay time constants differ by more than two orders of magnitude (~ 6 ns and 1.6μ s for the singlet and triplet respectively), the background rejection power, obtained by measuring the prompt fraction of S1, is larger than 10^7 in the WIMP ROI [5].

The cost of using (atmospheric) liquid argon is the high intrinsic radioactivity, due to ^{39}Ar , activated by cosmic rays in natural argon. The typical activity of this β -emitter (with endpoint at 565 keV and 269 years half-life) in atmospheric argon is 1 Bq/kg [6] and represents the limiting factor for the scaling of a liquid argon TPC. The solution proposed by the DarkSide collaboration is the use of argon extracted from underground sources, where it has been shielded from cosmic rays during thousands of years.

3. – The DarkSide program

The DarkSide program aims to perform a background-free WIMP search by using a dual-phase liquid argon detector with a 100 ty exposure. Some of the key points of the program are the exploitation of pulse shape discrimination (PSD) for ER background rejection; the use of argon extracted from underground sources to reduce the ^{39}Ar activity and the implementation of an active veto to tag neutron induced NR.

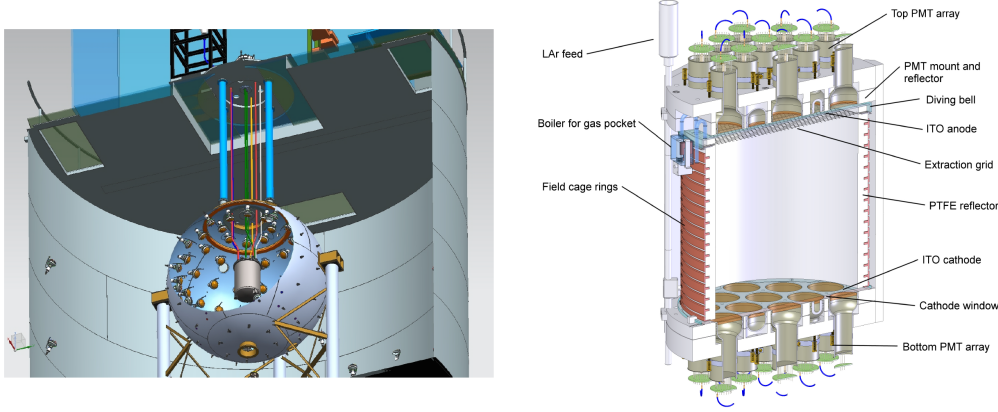
The current phase of the experiment, DarkSide-50, demonstrated the exceptional ER background rejection achievable in liquid argon, by running the detector with an atmospheric argon fill during several months. Moreover, with a six years effort, the DarkSide Collaboration successfully managed to extract a first > 150 kg batch of underground argon from an CO_2 well in Cortez, Colorado, [7] and DarkSide-50 is currently running with an underground argon fill. The measured depletion factor is sufficient to guarantee the operation of a multi-ton detector. Both these aspects will be addressed in the next sections.

The active veto system of DarkSide-50 is described in detail in [8]. It is 4π liquid scintillator detector, conceived to have high efficiency ($>99.1\%$) for neutron capture (achieved thanks to a boron loading) and detection of the capture products. Neutrons are

The design of the next phase of the experiment, DarkSide-20k, is currently being finalized. The experimental setup will reflect the current DarkSide-50 layout, and will be discussed in the last section.

3.1. The DarkSide-50 experiment. – The DarkSide-50 cylindrical dual-phase TPC contains ~ 50 kg of liquid argon. Two arrays of 19 PMTs each look inside the sensitive

Fig. 1. – A sketch of the DarkSide-50 three nested detectors (left) and a cutaway drawing of the DarkSide-50 TPC (left).



volume through two quartz windows. All the inner walls of the TPC are coated with TPB, to shift the VUV scintillation light in the visible range. A uniform electric field (nominal intensity of 200 V/cm) allows the ionization charges to drift along the vertical direction. A 1 cm thick gas layer is created on top of the liquid and a 2.8 kV/cm electric field allows the S2 formation by extracting and accelerating the electrons in the gas.

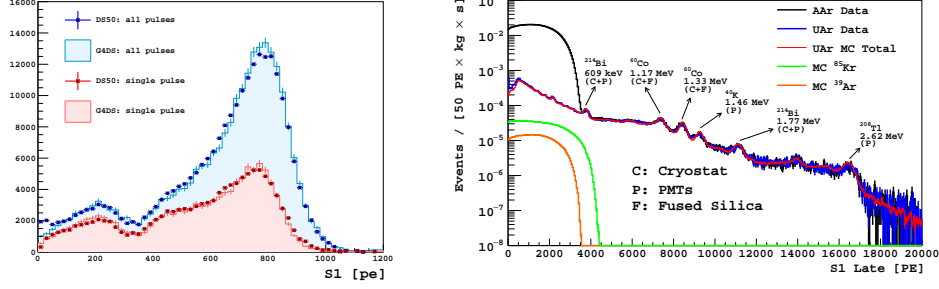
The experimental setup, shown in fig. 1, consists of three nested detectors: the cryostat hosting the TPC is placed inside a 4 m diameter sphere, in turn inside a 10 m diameter, 11 m tall water tank. The outer detector, equipped with 80 PMTs, acts as veto for cosmic muons. The sphere, filled with liquid scintillator and observed by 110 PMTs, is the active neutron veto. The system is currently running at LNGS and the acquired data correspond to more than one year lifetime. The first 50 days lifetime data acquisition campaign was performed with an Atmospheric Argon (AAr) fill and the results are reported in [5]. In April 2015 the detector was successfully filled with Underground Argon (UAr) and the planned 3 years data taking got started. The results of the analysis of a 70 days lifetime subset of the acquired data is reported in [9].

The data taking is stable and no significant degradation of the detector performance were observed after the UAr filling: the measurements of S1 light yield (~ 7.3 pe/keV at the nominal field of 200 V/cm) and electron lifetime (> 5 ms) are measured and periodically monitored by means of the injection of ^{83m}Kr in the liquid argon.

3.2. The DarkSide-50 Results. – The DarkSide WIMP search aims to identify single-sited interactions in the sensitive volume without a coincident signal in the vetoes. The data selection criteria are described in detail in [5]. To distinguish nuclear from electron recoil, the f_{90} variable, defined as the fraction of S1 collected in the first 90 ns of the signal, is used as PSD parameter. The intersection of the 90% NR acceptance curve with the leakage prediction contour, corresponding to an ER leakage of less than 0.1 events in the full exposure, describe the contours of the WIMP search region.

During the AAr run, a large statistics of ER data in the WIMP energy region was collected ($> 10^7$), but all of them were rejected by PSD. This results sets a lower limit on the ER rejection achievable thanks to the PSD. In addition to this, three NR candidates were rejected because a coincident signal was found in the vetoes.

Fig. 2. – The data-MC S1 spectra comparison for the ^{57}Co calibration source (left) and the spectral fit with MC components of the full DarkSide-50 S1_{late} spectrum. The S1_{late} variable is defined as the S1 tail integral to avoid the electronics saturation.



The UAr dataset was used to measure the depletion factor of ^{39}Ar in the UAr with a MC based fit. G4DS, the GEANT4-based simulation of the DarkSide experiment, is able to reproduce the TPC response at the %-level and includes an effective model for the ionization and scintillation mechanisms in liquid argon. It is tuned on AAr data and the calibration is validated with external calibration sources (as shown in fig. 2 left). We fit the S1 spectrum with MC components and found a reduction of the ^{39}Ar activity of 1400 ± 200 , as presented in fig. 2 right. In addition to this, we discovered an unexpected contamination of ^{85}Kr , which decays through β^- emission with endpoint at 687 keV. The presence of ^{85}Kr was later confirmed by looking at the 0.43% BR β^- decay to ^{85m}Rb , with a γ delayed coincidence. The two independent predictions on the ^{85}Kr activity agree within the errors.

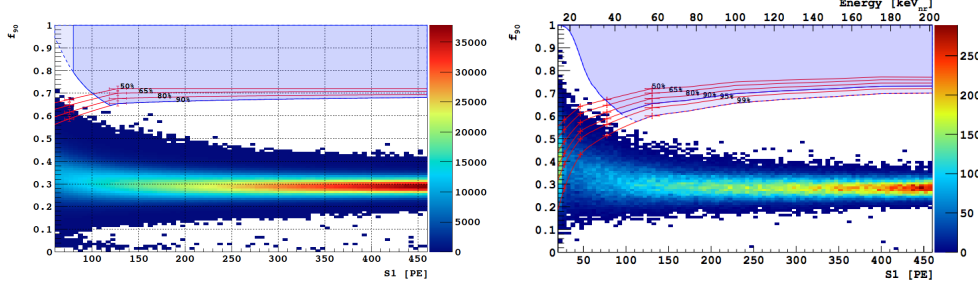
As expected from the AAr result, no ER event is leaking in the WIMP search region drawn for the UAr WIMP search. The acquired statistics is presented in fig. 3 for both the datasets. The 90% CL upper limit on the WIMP-nucleon cross section, derived from the AAr and UAr combined exposure, background-free, null results is shown in fig. 4, together with the projected sensitivity for 3 years of data taking. The limit is $2.0 \times 10^{-44} \text{ cm}^2$ for a 100 GeV/c² mass WIMP.

3.3. The Future: DarkSide-20k. – The next phase of the DarkSide experiment consists in building a 23 t active (20 t fiducial) mass TPC to reach 100 ty exposure. As already mentioned, the experimental setup will reflect the current DarkSide-50 layout: the TPC will be hosted inside a liquid scintillator veto (8 m diameter) in turn placed inside a 12 m diameter water tank.

The TPC light readout system will be improved, by using SiPM instead of traditional PMTs. This choice is beneficial in terms of internal radioactivity (less material around the active volume) and collection of the light. With SiPMs is possible to achieve both higher photo-detection efficiency (PDE) and better geometrical coverage compared to PMTs. To reduce the number of channels down to a manageable number, they will be grouped in $5 \times 5 \text{ cm}^2$ tiles. Several ongoing R&D and the preliminary tests on prototype tiles are giving promising results (for instance in terms of PDE, dark count rate, time resolution, gain).

The optical simulation of the TPC, tuned on DarkSide-50, can be propagated to the new geometry: the new readout system implies an increased S1 light yield of $\sim 10 \text{ pe/keV}$,

Fig. 3. – Result of the dark matter search for the AAr (left) and UAr (right) campaigns. The fraction of S1 in the first 90 ns of the signal (f_{90}) is the PSD parameter. The nuclear recoil equivalent energy scale on top of the right plot is for illustrative purposes only. In both the dataset, no event is found in the WIMP search region (blue shaded area).



feature that will improve the PSD rejection power.

Assuming the ^{39}Ar depletion factor and the γ radioactivity levels measured in DarkSide-50 we expect the ER background to be efficiently removed by the PSD. Particular attention has been devoted to the NR background. G4DS simulations of (α, n) neutrons and from all the detectors materials show that, thanks to the neutron veto, the NR background can be maintained below 0.1 events in the full exposure with a correct choice of the detector materials. Moreover, the cosmic muon induced neutron background will be negligible. The only irreducible background, due to CNNS⁽¹⁾, is predicted to be as large as 1.6 events in the full exposure. The projected sensitivity of DarkSide-20k, based on the background-free hypothesis, is shown in fig. 4.

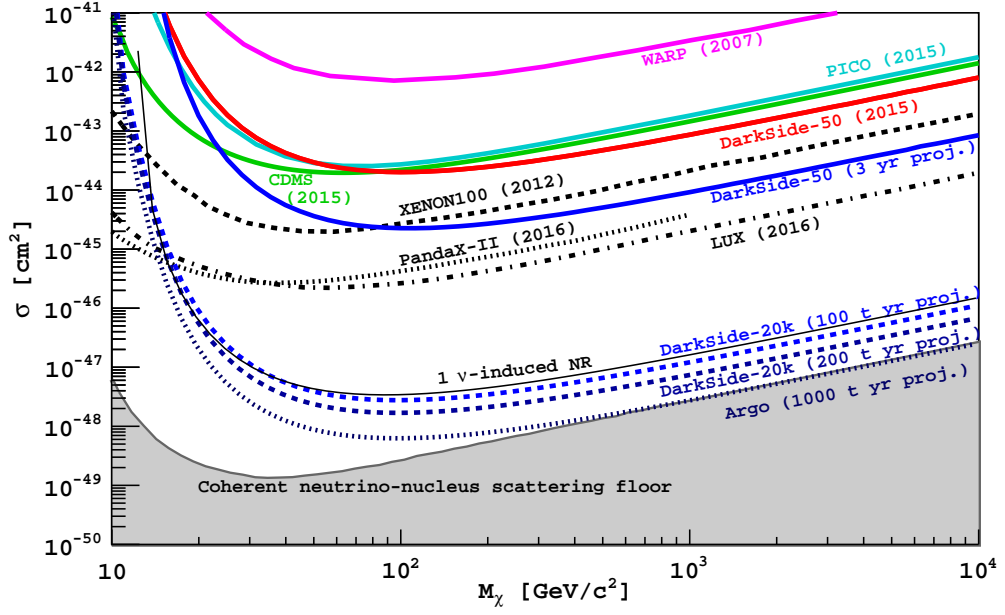
4. – Conclusions

I reported in this work about the status and perspective of the DarkSide experiment at LNGS. DarkSide-50, the current phase of the experiment, a dual-phase TPC filled with underground argon is currently running. To date, the background-free null result sets a limit on the WIMP-nucleon cross section of $2.0 \times 10^{-44} \text{ cm}^2$ for a WIMP mass of $100 \text{ GeV}/c^2$. Moreover, the first data taking campaign, obtained with an atmospheric argon fill, demonstrated the high ER rejection power achievable in argon. The first data collected with the underground argon target allowed instead the measurement of the depletion factor of ^{39}Ar with respect to the atmospheric argon.

The combination of these results represents the basis for the next phase of the experiment: DarkSide-20k. The detector is designed to have a 20 t sensitive mass and to reach 100 ty background-free exposure. The data taking is expected to start by 2021.

⁽¹⁾ Cosmic neutrino-nucleon scattering.

Fig. 4. – Spin-independent WIMP-nucleon cross section exclusion plot. The current DarkSide-50 exclusion curve (solid red), computed comparing AAr and UAr exposures, is compared to the xenon-based experiment limits (dotted black) and to the 3 years projected sensitivity (solid blue). The DarkSide-20k projected sensitivity is also shown (dotted blue) along with the 1 CNNS event curve (solid black).



REFERENCES

- [1] ADE P. A. R. *et al.*, *A&A*, **594** (2015) A13.
- [2] TAN A. *et al.*, *Phys. Rev. Lett.*, **117** (2016) 121303.
- [3] APRILE E. *et al.*, *JCAP*, **2016** (2016) 027.
- [4] MOUNTS B. J. *et al.*, *arXiv:1703.09144*, (2017) .
- [5] AGNES P. *et al.*, *Phys. Lett. B*, **743** (2015) 456 .
- [6] BENETTI P. *et al.*, *NIM A*, **574** (2007) 83 .
- [7] BACK H. O. *et al.*, *arXiv:1204.6024*, (2012) .
- [8] AGNES P. *et al.*, *JINST*, **11** (2016) P03016.
- [9] AGNES P. *et al.*, *Phys. Rev. D*, **93** (2016) 081101.